Satellites of simulated galaxies: survival, merging and their relation to the dark and stellar haloes

Laura V. Sales,[1,2]★ Julio F. Navarro,[3,4]† Mario G. Abadi[1,2,3] and Matthias Steinmetz[5]

[1]*Observatorio Astronómico, Universidad Nacional de Córdoba, Laprida 854, 5000 Córdoba, Argentina*
[2]*Instituto de Astronomía Teórica y Experimental, Conicet, Argentina*
[3]*Department of Physics and Astronomy, University of Victoria, Victoria, BC V8P 5C2, Canada*
[4]*Max-Planck Institut für Astrophysik, Karl-Schwarzschild Strasse 1, Garching, D-85741, Germany*
[5]*Astrophysikalisches Institut Potsdam, An der Sternwarte 16, Potsdam 14482, Germany*

ABSTRACT

We study the population of satellite galaxies formed in a suite of *N*-body/gasdynamical simulations of galaxy formation in a Λ cold dark matter universe. The simulations resolve nearly 10 most luminous satellites around each host, and probe systems up to six or seven magnitudes fainter than the primary. We find little spatial or kinematic bias between the dark matter and the satellite population. The radius containing half of all satellites is comparable to the half-mass radius of the dark matter component, and the velocity dispersion of the satellites is a good indicator of the virial velocity of the halo; $\sigma_{sat}/V_{vir} \sim 0.9 \pm 0.2$. Applied to the Local Group, this result suggests that the virial velocity of the Milky Way and M31 might be substantially lower than the rotation speed of their disc components; we find $V_{vir}^{MW} \sim 109 \pm 22$ km s^{-1} and $V_{vir}^{M31} \sim 138 \pm 35$ km s^{-1}, respectively, compared to $V_{rot}^{MW} \sim 220$ km s^{-1} and $V_{rot}^{M31} \sim 260$ km s^{-1}. Although the uncertainties are large, it is intriguing that both estimates are significantly lower than expected from some semi-analytic models, which predict a smaller difference between V_{vir} and V_{rot}. The detailed kinematics of simulated satellites and dark matter are also in good agreement: both components show a steadily decreasing velocity dispersion profile and a mild radial anisotropy in their velocity distribution. By contrast, the stellar halo of the simulated galaxies, which consists predominantly of stellar debris from *disrupted* satellites, is kinematically and spatially distinct from the population of *surviving* satellites. This is because the survival of a satellite as a self-bound entity depends sensitively on mass and on time of accretion and surviving satellites are significantly biased toward low-mass systems that have been recently accreted by the galaxy. Our results support recent proposals for the origin of the systematic differences between stars in the Galactic halo and in Galactic satellites: the elusive 'building blocks' of the Milky Way stellar halo were on average more massive, and were accreted (and disrupted) earlier than the population of dwarfs that has survived self-bound until the present.

Key words: galaxies: evolution – galaxies: formation – galaxies: haloes.

1 INTRODUCTION

The satellite companions of bright galaxies are exceptionally useful probes of the process of galaxy formation. Studies of the dynamics of satellites around bright galaxies, for example, have provided incontrovertible evidence for the ubiquitous presence of massive dark haloes surrounding luminous galaxies, a cornerstone of the present galaxy formation paradigm. Following the pioneering work of Holmberg (1969), Zaritsky et al. (1993, 1997) compiled perhaps the first statistically sound sample of satellite-primary systems with accurate kinematics, and were able to provide persuasive evidence that the dark matter haloes hinted at by the flat rotation curves of spiral galaxies (Sofue & Rubin 2001, and references therein) truly dwarf the mass of the luminous component and extend well beyond the luminous radius of the central galaxy.

Satellite dynamical studies have entered a new realm since the advent of large redshift surveys, such as the two-degree field Galaxy Redshift Survey (2dfGRS) (Colless et al. 2001) and the Sloan Digital Sky Survey (SDSS) (York et al. 2000; Strauss et al. 2002), which have increased many fold the number of primary-satellite systems

★E-mail: lsales@oac.uncor.edu
†Fellow of the Canadian Institute for Advanced Research.

known. Recent work based on these data sets have corroborated and extended the results of Zaritsky et al., and their conclusions now appear secure. The dynamics of satellites confirm (i) that dark matter haloes extend to large radii, (ii) that more massive haloes surround brighter galaxies and (iii) that early-type galaxies are surrounded by haloes about twice as massive as late-type systems of similar luminosity (McKay et al. 2002; Prada et al. 2003; Brainerd 2004b; van den Bosch et al. 2005; see Brainerd 2004a for a recent review).

Satellites may also be thought of as probes of the faint-end of the luminosity function. After all, satellite galaxies are, by definition, dwarf systems, thought to be themselves surrounded by their own low-mass dark matter haloes. These low-mass haloes are expected to be the sites where the astrophysical processes that regulate galaxy formation (i.e. feedback) operate at maximum efficiency. Thus, the internal structure, star formation history and chemical enrichment of satellites provide important constraints on the process of galaxy formation in systems where theoretical models predict a highly non-trivial relation between dark mass and luminosity (see e.g. White & Rees 1978; Kauffmann, White & Guiderdoni 1993; Cole et al. 1994; see as well Cole et al. 2000; Benson, Frenk & Sharples 2002a for a more detailed list of references).

The anticipated highly non-linear mapping between dark matter and light at the faint-end of the luminosity function is perhaps best appreciated in the satellite population of the Local Group, where relatively few known satellites stand in contrast with the *hundreds* of 'substructure' cold dark matter (CDM) haloes of comparable mass found in cosmological *N*-body simulations (Klypin et al. 1999; Moore et al. 1999). Possible resolutions of this 'satellite crisis' have been discussed by a number of authors, and there is reasonably broad consensus that it originates from inefficiencies in star formation caused by the combined effects of energetic feedback from evolving stars and by the diminished supply of cold gas due to reionization (see e.g. Kauffmann et al. 1993; Bullock, Kravtsov & Weinberg 2000; Somerville, Primack & Faber 2001; Benson, Frenk & Sharples 2002a). These effects combine to dramatically reduce the star formation activity in substructure haloes, and can reconcile, under plausible assumptions, the substructure halo mass function with the faint-end of the satellite luminosity function (Stoehr et al. 2002; Kazantzidis et al. 2004; Peñarrubia, McConnachie & Navarro 2007).

The price paid for reconciling CDM substructure with the Local Group satellite population is one of simplicity, as the 'feedback' processes invoked involve complex astrophysics that is not yet well understood nor constrained. It is not yet clear, for example, whether the brighter satellites inhabit the more massive substructures, or whether, in fact, there is even a monotonic relation between light and mass amongst satellites. This issue is further complicated by the possibility that a substantial fraction of a satellite's mass may have been lost to tides. Tidal stripping is expected to affect stars and dark matter differently, complicating further the detailed relation between light and mass in substructure haloes (Hayashi et al. 2003; Kravtsov, Gnedin & Klypin 2004; Strigari, Bullock & Kaplinghat 2007a; Strigari, Kaplinghat & Bullock 2007b).

These uncertainties hinder as well the interpretation of satellites as relics of the hierarchical galaxy assembly process, and consensus has yet to emerge regarding the severity of the biases that the various effects mentioned above may engender. Do the spatial distribution of satellites follow the dark matter? Are the kinematics of the satellite population substantially biased relative to the dark matter's? Have satellites lost a substantial fraction of their stars/dark matter to stripping? Are surviving satellites fair tracers of the population of accreted dwarfs?

Of particular interest is whether satellites may be considered relics of the 'building blocks' that coalesced to form the early Galaxy. Indeed, the stellar halo of the Milky Way is regarded, in hierarchical models, to consist of the overlap of the debris of many accreted satellites which have now merged and mixed to form a kinematically hot, monolithic stellar spheroid (Searle & Zinn 1978; Bullock & Johnston 2005; Abadi, Navarro & Steinmetz 2006; Moore et al. 2006). A challenge to this view comes from detailed observation of stellar abundance patterns in satellite galaxies in the vicinity of the Milky Way. At a given metallicity, the stellar halo (at least as sampled by stars in the solar neighbourhood) is systematically more enriched in α-elements than stars in Galactic satellites (Fuhrmann 1998; Shetrone, Côté & Sargent 2001; Shetrone et al. 2003; Venn et al. 2004), a result that remains true even when attempting to match stars of various ages or metallicities (Unavane, Wyse & Gilmore 1996; Gilmore & Wyse 1998; Pritzl, Venn & Irwin 2005). Can hierarchical models explain why satellites identified today around the Milky Way differ from the ones that fused to form the Galactic halo? Preliminary clues to these questions have been provided by the semi-analytic approach of Bullock, Johnston and collaborators (Bullock & Johnston 2005; Font et al. 2006a,b), who argue that hierarchical models predict naturally well-defined distinctions between the halo and satellite stellar populations. Detailed answers, however, depend critically on which and when substructure haloes are 'lit up' and how they evolve within 'live' dark matter haloes. These are perhaps best addressed with direct numerical simulation that incorporates the proper cosmological context of accretion as well as the gasdynamical effects of cooling and star formation in an evolving population of dark matter haloes. The study we present here aims to address these issues by analysing the properties of the satellite population of L_* galaxies simulated in the ΛCDM scenario. We briefly introduce the simulations in Section 2, analyse and discuss them in Section 3 and conclude with a summary in Section 4.

2 THE NUMERICAL SIMULATIONS

Our suite of eight simulations of the formation of L_* galaxies in the ΛCDM scenario is the same discussed recently by Abadi et al. (2006). The simulations are similar to the one originally presented by Steinmetz & Navarro (2002), and have been analysed in detail in several recent papers, which the interested reader may wish to consult for details on the numerical setup (Abadi et al. 2003a,b; Meza et al. 2003, 2005; Navarro, Abadi & Steinmetz 2004).

Briefly, each simulation follows the evolution of a small region of the universe chosen so as to encompass the mass of an L_* galaxy system. This region is chosen from a large periodic box and re-simulated at higher resolution preserving the tidal fields from the whole box. The simulation includes the gravitational effects of dark matter, gas and stars, and follows the hydrodynamical evolution of the gaseous component using the Smooth Particle Hydrodynamics (SPH) technique (Steinmetz 1996). We adopt the following cosmological parameters for the ΛCDM scenario: $H_0 = 65 \text{ km s}^{-1} \text{ Mpc}^{-1}$, $\sigma_8 = 0.9$, $\Omega_\Lambda = 0.7$, $\Omega_{CDM} = 0.255$, $\Omega_{bar} = 0.045$, with no tilt in the primordial power spectrum.

All simulations start at redshift $z_{init} = 50$, have force resolution of the order of 1 kpc and the mass resolution is chosen so that each galaxy is represented on average, at $z = 0$, with $\sim 50\,000$ gas/dark matter particles and $\sim 125\,000$ star particles. Each re-simulation follows a single $\sim L_*$ galaxy in detail, and resolves a number of smaller, self-bound systems we will call generically 'satellites'. We will hereafter refer to the main galaxy indistinctly as 'primary' or 'host'.

Gas is allowed to turn into stars at rates consistent with the empirical Schmidt-like law of Kennicutt (1998) in collapsed regions at the centre of dark matter haloes. Because star formation proceeds efficiently only in high-density regions, the stellar components of primary and satellites are strongly segregated spatially from the dark matter. We include the energetic feedback of evolving stars, although its implementation mainly as a heating term on the (dense) gas surrounding regions of active star formation implies that most of this energy is lost to radiation and that feedback is ineffective at curtailing star formation. The transformation of gas into stars thus tracks closely the rate at which gas cools and condenses at the centre of dark matter haloes. This results in an early onset of star-forming activity in the many progenitors of the galaxy that collapse at high redshift, as well as in many of the satellite systems we analyse here.

Another consequence of our inefficient feedback algorithm is that gas cooling and, therefore, star formation proceed with similar efficiency in all well-resolved dark matter haloes, irrespective of their mass. As a result, the total stellar mass of a satellite correlates quite well with the 'original' mass of its progenitor dark halo; i.e. the total mass of the satellite before its accretion into the virial radius of its host. We define the *virial* radius, r_{vir}, of a system as the radius of a sphere of mean density $\Delta_{vir}(z)$ times the critical density for closure. This definition defines implicitly the virial mass, M_{vir}, as that enclosed within r_{vir}, and the virial velocity, V_{vir}, as the circular velocity measured at r_{vir}. Quantities characterizing a system will be measured within r_{vir}, unless otherwise specified. The virial density contrast, $\Delta_{vir}(z)$, is given by $\Delta_{vir}(z) = 18\pi^2 + 82f(z) - 39f(z)^2$, where $f(z) = [\Omega_0(1+z)^3/(\Omega_0(1+z)^3 + \Omega_\Lambda))] - 1$ and $\Omega_0 = \Omega_{CDM} + \Omega_{bar}$ (Bryan & Norman 1998). $\Delta_{vir} \sim 100$ at $z = 0$.

It is likely that improvements to our feedback algorithms may lead to revisions in the efficiency and timing of star formation in these galaxies, and especially in the satellites, but we think our results will nonetheless apply provided that these revisions do not compromise the relatively simple relation between stellar mass and halo mass that underpins many of our results. For example, we expect that modifications of the star formation algorithm will affect principally the number, age and chemical composition of stars, rather than the dynamical properties of the satellites. This is because the latter depend mainly on the mass, orbit and timing of the merging progenitors, which are largely dictated by the assumed cosmological model. These properties are less sensitive to the complex astrophysics of star formation and feedback, and therefore our analysis focuses on the kinematics and dynamical evolution of the satellite population around the eight galaxies in our simulation suite.

3 RESULTS AND DISCUSSION

3.1 Characterization of the satellite population

Fig. 1 shows the spatial distribution of all star particles in four of our simulated galaxies. Stars are assigned to one of three components and coloured accordingly. Particles in cyan are 'in situ' stars, i.e. stars that formed in the main progenitor of the primary galaxy. Stars in red formed in satellites that have since been accreted and fully disrupted by the tidal field of the galaxy. Stars in yellow formed in systems that survive as recognizable self-bound satellites until $z = 0$. As discussed in detail by Abadi et al. (2006), the tidal debris of fully disrupted satellites makes up the majority of the smooth outer stellar halo component. 'In situ' stars, on the other hand, dominate the inner galaxy, whereas surviving satellites are easily identifiable as overdense, tightly bound clumps of stars.

In practice, we identify satellite systems using a friends-of-friends algorithm to construct a list of potential stellar groupings, each of which is checked to make sure that (i) they are self-bound and (ii) they contain at least 35 star particles. This minimum number of stars (which corresponds roughly to ∼0.03 per cent of the stellar mass of the primary at $z = 0$) is enough to ensure the reliable identification of the satellite at various times and the robust measurement of their orbital properties, but is insufficient to study the internal structure of the satellite. The satellite identification procedure is run for all snapshots stored for our simulations, allowing us to track the evolution of individual satellites.

With these constraints, our simulations resolve, at $z = 0$, an average of about 10 satellites within the virial radius of each simulated galaxy. The cumulative luminosity distribution of these satellites (computed in the V band[1] for ease of comparison with data available for the Local Group satellites) is shown in Fig. 2. The brightest satellite is, on average, about ∼12 per cent as bright as the primary, in reasonable agreement with the most luminous satellite around the Milky Way and M31: the LMC and M33 are, respectively, 11 and 8 per cent as bright as the MW and M31 (van den Bergh 1999).

At brightnesses below 0.2 per cent of L_{host}, the number of simulated satellites levels off as a result of numerical limitations. Independent tests (Abadi et al., in preparation) show that this brightness limit corresponds to where satellite identification in the simulations becomes severely incomplete. We note that this limitation precludes us from addressing the 'satellite crisis' alluded to in Section 1: our simulations lack the numerical resolution needed to resolve the hundreds of low-mass substructure haloes found in higher-resolution CDM simulations. On average, the 10th brightest satellite in our simulations is ∼5.6 mag fainter than the primary; for comparison, the MW and M31 have only two and five satellites as bright as that.

Given the small number of systems involved and the considerable scatter from simulation to simulation (the number of bright satellites ranges from 4 to 21 in our eight simulations), we conclude that there is no dramatic discrepancy between observations and simulations at the bright end of the satellite luminosity function. Applying our results to the full Local Group satellite population, including, in particular, the extremely faint dwarfs being discovered by panoramic surveys of M31 and by the SDSS (Zucker et al. 2004, 2006; Willman et al. 2005; Belokurov et al. 2006, 2007; Martin et al. 2006; Irwin et al. 2007; Majewski et al. 2007; Ibata et al. 2007), involves a fairly large extrapolation, and should be undertaken with caution (see e.g. Peñarrubia et al. 2007 for a recent discussion).

3.2 Spatial distribution

Fig. 1 shows that satellites are found throughout the virial radius of the host and that, unlike stars in the smooth stellar halo, satellites show little obvious preference for clustering in the vicinity of the central galaxy. This is confirmed in Fig. 3, where the solid circles show the number density profile of satellites, after rescaling their positions to the virial radius of each host and stacking all eight simulations. The dashed and dotted lines in this figure correspond, respectively, to the density profile of the stellar and dark matter haloes, scaled and stacked in a similar way. The vertical normalization of the satellite and stellar halo profiles is arbitrary, and has been chosen so that all profiles approximately match at $r \sim 0.15r_{vir}$.

---

[1] Luminosity estimates in various bands are made by convolving the masses and ages of star particles with standard spectrophotometric models (see e.g. Abadi et al. 2006 for details).
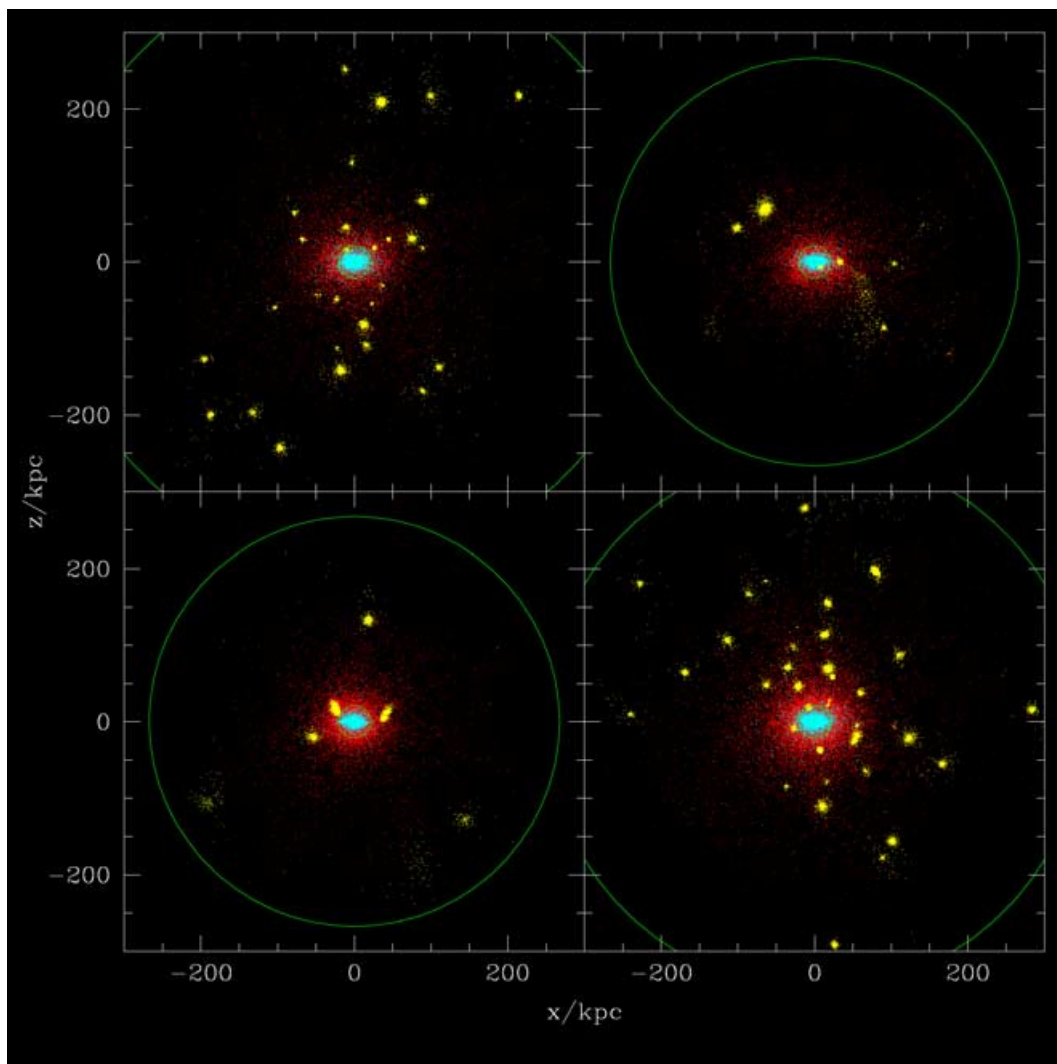
Figure 1. Spatial distribution of the stellar component of four of our simulated galaxies at $z = 0$. Each panel corresponds to a different simulation, projected so that the inner galaxy is seen approximately 'edge-on'. The virial radius of the system is marked by the outer green circle in each panel. The inner circle has a radius of 20 kpc, where most of the stars in each galaxy are found. Stars that have formed in satellites that survive as self-bound entities until $z = 0$ are shown in yellow. 'In situ' stars, i.e. those formed in the most massive progenitor of the galaxy, are shown in cyan, whereas those formed in satellites that have been accreted and disrupted by the main galaxy are shown in red. Note that the diffuse outer stellar halo reaches almost out to the virial radius, and consists almost exclusively of accreted stars. The inner galaxy, on the other hand, is dominated by stars formed 'in situ'.

There is little difference in the shape of the dark matter and satellite profiles: half of the satellites are contained within $\sim 0.37 r_{\mathrm{vir}}$, a radius similar to the half-mass radius of the dark matter, $\sim 0.3 r_{\mathrm{vir}}$. We conclude that, within the uncertainties, the satellites follow the dark matter. The stellar halo, on the other hand, is much more centrally concentrated than the dark matter and satellites; its half-mass radius is only $\sim 0.05 r_{\mathrm{vir}}$, as shown by the arrows in Fig. 3.

This result implies that the spatial distribution of simulated satellites is distinct from that of CDM substructure haloes, whose density profile is known to be significantly shallower than the dark matter's (Ghigna et al. 1998, 2000; Diemand, Moore & Stadel 2004; Gao et al. 2004). This suggests that the 'mapping' between dark and luminous substructure is highly non-trivial, as argued by Springel et al. (2001) and De Lucia et al. (2004). Our results, which are based on direct numerical simulation, validate these arguments and illustrate the complex relation between galaxies and the subhaloes in which they may reside (see also Kravtsov et al. 2004; Nagai & Kravtsov

2005; Gnedin et al. 2006; Weinberg et al. 2006; Libeskind et al. 2007). Luminous satellites are resilient to disruption by tides, and they can survive as self-bound entities closer to the primary, where substructures in dark matter-only simulations may quickly disrupt, as first pointed out by White & Rees (1978).

We conclude that using dark matter substructures to trace directly the properties of luminous satellites is likely to incur substantial and subtle biases which may be difficult to avoid. Models that attempt to follow the evolution of dark matter substructures and their luminous components are likely to fare better (see e.g. Bower et al. 2006; Croton et al. 2006). At the low-mass end, the inclusion of some treatment of the substructure mass loss and tidal shocks is needed to put in better agreement semi-analytic models with the results from numerical simulations (Taylor & Babul 2001; Benson et al. 2002b). Definitive conclusions will probably need to wait until realistic simulations with enhanced numerical resolution and improved treatment of star formation become available.
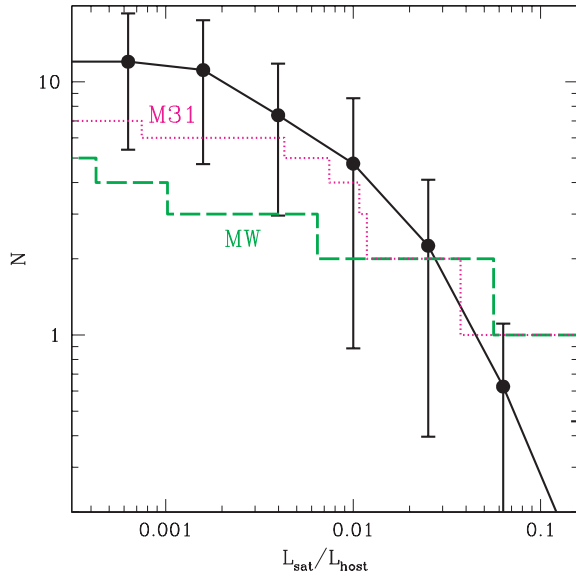
Figure 2. Cumulative luminosity distribution of simulated satellites (filled circles), averaged over our eight simulations, and compared with the Milky Way (blue dashed line) and M31 (red dotted curve) satellite systems. Satellite luminosities are scaled to the luminosity of the host. Error bars in the simulated data indicate Poisson uncertainties in the computation of the average. The flattening of the simulated satellite distribution below 0.1 per cent of the primary luminosity is due to numerical limitations. The Local Group data are taken from van den Bergh (1999). For the MW and M31 systems, we include only satellites at distances closer than 300 kpc from the central galaxy.
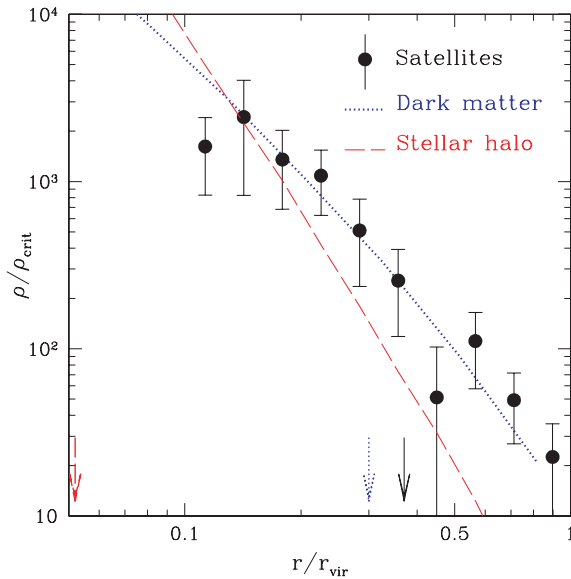
3.3 Kinematics

The likeness in the spatial distribution of satellites and dark matter anticipates a similar result for their kinematics. This is illustrated in Fig. 4, where the panels on the left-hand side show the spherical components of the satellites' velocities (in the rest frame of the host and scaled to its virial velocity) versus galactocentric distance (in units of the virial radius of the host). Velocity components are computed after rotating each system so that the z-axis (the origin of the polar angle θ) coincides with the rotation axis of the inner galaxy. The corresponding velocity distributions are shown by the thick solid lines in the panels on the right-hand side, and compared with those corresponding to the dark matter particles (dotted lines).

The velocity distribution of each component is reasonably symmetric and may be well approximated by a Gaussian, except perhaps for the satellites' V_ϕ-component, which is clearly asymmetric. This is a result of net rotation around the z-axis: the satellite population has a tendency to co-rotate with the galaxy's inner body which is more pronounced than the dark matter's. Indeed, we find that on average the specific angular momentum of satellites is ∼50 per cent higher than the dark matter, and a factor of ∼10 higher than the stellar halo. This result likely arises as a consequence of the accretion and survival biases discussed below; surviving satellites accrete late and from large turnaround radii, making them especially susceptible to the tidal torques responsible for spinning up the galaxy. The overall effect, however, is quite small, and rotation provides a negligible amount of centrifugal support to the satellite population.

The velocity dispersion of both satellites and dark matter particles drops steadily from the centre outwards, as shown in Fig. 5. The top
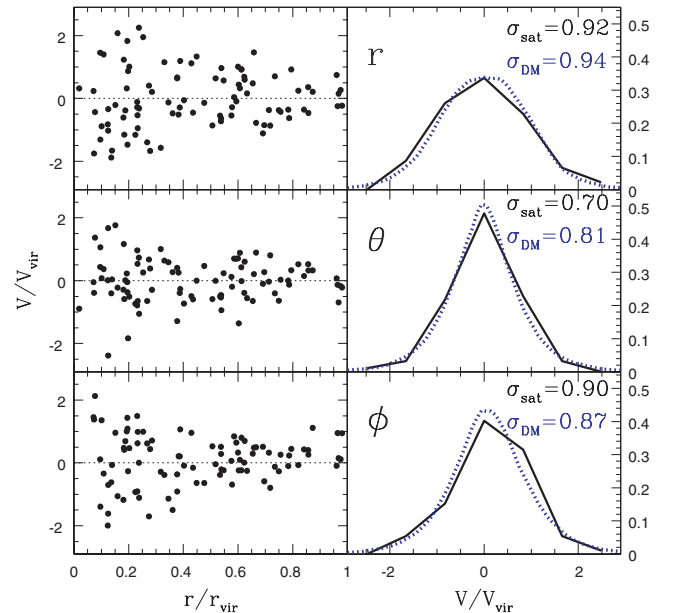

Figure 3. Number density profile of simulated satellites, after scaling their positions to the virial radius of each host and stacking all eight simulations (solid circles; error bars denote Poisson uncertainties associated with the total number of satellites in each radial bin). The dotted line corresponds to the average dark matter density profile, and the dashed line to the stars in the outer stellar halo. The vertical normalization for the satellite and stellar halo profiles has been chosen so that all profiles approximately coincide at $r \sim 0.15 r_{\rm vir}$. Note that the spatial distribution of satellites is similar to the dark matter, and that stars in the stellar halo are significantly more centrally concentrated. Arrows mark the radius containing half the objects in each component (see text for further discussion).

Figure 4. Spherical components of satellite velocities at $z = 0$ as a function of their distance to the centre of the host galaxy. Each system has been rotated so that the angular momentum of the inner galaxy is aligned with the direction of the z-coordinate axis. Positions and velocities have been scaled to the virial radius and velocity of each host halo. Panels on the right-hand side show the velocity distributions of the satellite population within $r_{\rm vir}$ (solid lines) and compare it to the dark matter particles (dotted lines). The velocity dispersions are given in each panel. Note the slight asymmetry in the satellites' V_ϕ velocity distribution, which results from the net co-rotation of satellites around the primary.
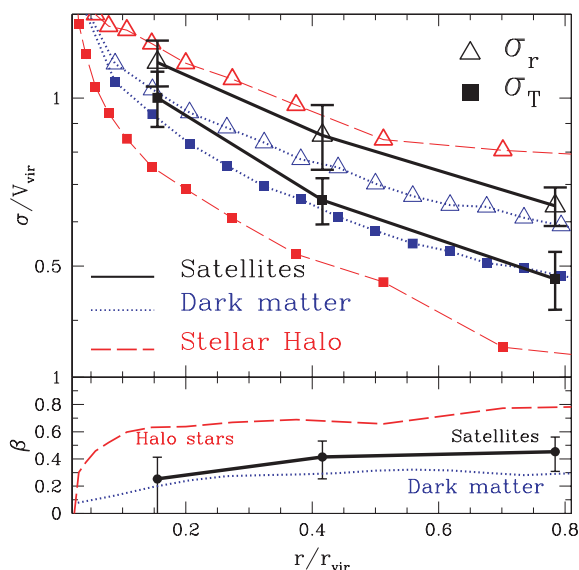
Figure 5. Top panel: radial and tangential velocity dispersion profiles of satellites, dark matter and stellar halo computed after scaling to virial values and stacking all simulations in our series. Bottom panel: anisotropy parameter as a function of radius for the satellite population, compared with dark matter particles and with the stellar halo. Note that satellites are only slightly more radially anisotropic than the dark matter and kinematically distinct from the stellar halo.

panel shows that the drop is similar in all components, and that the velocity dispersion decreases from its central value by a factor of ~ 2 at the virial radius. This figure also shows that the velocity distribution is radially anisotropic, and that the anisotropy becomes more pronounced in the outer regions. The trends are again similar for satellites and dark matter, rising slowly with radius and reaching $\beta \sim 0.4$ at the virial radius. (The anisotropy parameter, β, is given by $\beta = 1 - (\sigma_t^2/2\sigma_r^2)$, where σ_r is the radial velocity dispersion and $\sigma_t = \sqrt{(\sigma_\phi^2 + \sigma_\theta^2)/2}$ is the tangential velocity dispersion.)

The stellar halo, on the other hand, is kinematically distinct from the satellites and from the dark matter. Overall, its velocity dispersion is lower, and its anisotropy is more pronounced, rising steeply from the centre outwards and becoming extremely anisotropic ($\beta \sim 0.8$) in the outer regions. As discussed in detail by Abadi et al. (2006), this reflects the origin of the stellar halo as debris from satellite disruption, which occur at small radii, where tidal forces are maximal. Stars lost during disruption (merging) events and that now populate the outer halo must therefore be on rather eccentric orbits, as witnessed by the prevalence of radial motions in Fig. 5. The kinematical distinction between satellites and stellar halo thus suggests that few halo stars have been contributed by stripping of satellites that have survived self-bound until the present. We will return to this issue below.

3.4 Application to the local group

The lack of strong kinematical bias between satellites and dark matter may be used to estimate the virial velocity of the Milky Way and M31. For example, assuming that the radial velocity dispersion of the satellites is related to the virial velocity by $\sigma_r \sim 0.9\,(\pm 0.2)\,V_{vir}$ (see Fig. 4; the uncertainty is just the rms scatter from our eight simulations), we obtain $V_{vir}^{MW} \sim 109 \pm 22$ km s^{-1} from the ~ 99 km s^{-1} Galactocentric radial velocity dispersion of the eleven brightest satellites (see e.g. the compilation of van den Bergh 1999).

The same procedure may be applied to M31 satellites. Taking into account projection effects, we find that the line-of-sight satellite velocity dispersion is $\sigma_{los} \sim 0.8\,(\pm 0.2)\,V_{vir}$. Taking the 16 brightest satellites within 300 kpc from the centre of M31, we find $\sigma_{los} \sim 111$ km s^{-1}, implying $V_{vir}^{M31} \sim 138 \pm 35$ km s^{-1}. We use here the compilation of McConnachie & Irwin (2006), complemented with data for And XIV from Majewski et al. (2007), and for And XII from Chapman et al. (2007).

These results imply that the virial radius of the Milky Way is $r_{vir}^{MW} \sim 240$ kpc. Our simulations predict that half of the brightest satellites should be enclosed within ~ 90 kpc, which compares favourably with observations: half of the eleven brightest satellites are within ~ 90.1 kpc from the centre of the Milky Way. Contrary to the arguments of Taylor, Silk & Babul (2005), no substantial bias between satellites and dark matter is required to explain the MW satellite spatial distribution, provided that one accepts a virial radius as small as ~ 240 kpc.

The same argument, applied to M31, suggests that half of the 16 satellites within its virial radius ($r_{vir}^{M31} \sim 300$ kpc) must be within ~ 111 kpc, compared with the observational value of ~ 165 kpc. Note that these radii are actual distances to M31, rather than projections.

Despite the sizable statistical uncertainty inherent to the small number of satellites in these samples, it is interesting that both of the virial velocity estimates mentioned above are significantly lower than the rotation speed measured for these galaxies in the inner regions; $V_{rot}^{MW} \sim 220$ km s^{-1} and $V_{rot}^{M31} \sim 260$ km s^{-1}. These low virial velocity estimates are in line with recent work that advocates relatively low masses for the giant spirals in the Local Group (Klypin, Zhao & Somerville 2002; Abadi, Navarro & Steinmetz 2006; Seigar, Barth & Bullock 2006; Smith et al. 2006).

If confirmed, this would imply that the circular velocity should drop steadily with radius in the outer regions of these galaxies. As discussed by Abadi et al. (2006), this may be the result of 'adiabatic contraction' of the dark matter halo following the assembly of the luminous galaxy. However, such result may be difficult to reconcile with semi-analytic models of galaxy formation, which favour a better match between V_{rot} and V_{vir}. Croton et al. (2006) argue that V_{rot} should be similar to the maximum circular velocity of the dark matter halo, which is only about ~ 20 per cent larger than V_{vir} for typical concentrations. It is possible that taking into account the effects of the adiabatic contraction and including the self-gravity of the baryon material might induce a large scatter and allow rotation speeds as high as $V_{rot} \sim 1.5$–2 times V_{vir} (A. Benson, private communication). Final word on this issue needs further data to place better constraints on the mass of the halo of the Local Group spirals at large distances, as well as improved semi-analytic modelling that re-examines critically the response of the dark halo to the formation of the luminous galaxy. At least from the observational point of view, the steady pace of discovery of new satellites of M31 and MW facilitated by digital sky surveys implies that it should be possible to revisit this issue in the near future with much improved statistics.

3.5 Satellite evolution

3.5.1 Merging and survival

Satellites are affected strongly by the tidal field of the primary, and evolve steadily after being accreted into the halo of the host galaxy. This is illustrated in Fig. 6, where the upper panel shows the evolution of the galactocentric distance for two satellites in one of our simulations. These two satellites follow independent accretion paths into the halo of the primary galaxy; after initially drifting
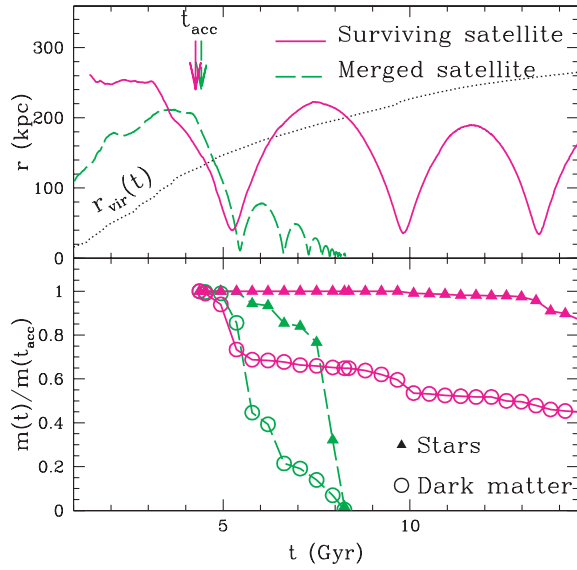
Figure 6. Top panel: orbital evolution of two satellites, chosen to illustrate the case of a system that merges quickly with the primary and of another that survives as a self-bound entity until $z = 0$. Curves show the distance from the primary to the self-bound stellar core of the satellite as a function of time. The dotted line shows the evolution of the virial radius of the primary galaxy, and the arrow indicates the time, t_{acc}, when the satellites are first accreted into the primary's halo. Although both satellites are accreted more or less at the same time, they are not a physical pair and evolve independently. Bottom panel: the evolution of the satellites' bound mass of stars and dark matter, normalized to the values computed at the time of accretion. Note that the stellar component is much more resilient to the effect of tides.

away from the galaxy due to the universal expansion, they reach a turnaround radius of a few hundred kpc and are then accreted into the virial radius of the primary at similar times, ~4.5 Gyr after the big bang ($z \sim 1.5$). The accretion is indicated by the intersection between the trajectory of each satellite in the upper panel of Fig. 6 and the dotted line, which shows the evolution of the virial radius of the main progenitor of the primary.

We define the time that the satellite first enters the virial radius of the primary as the *accretion time*, t_{acc} or z_{acc}, if it is expressed as a redshift. Because masses, radii and other characteristic properties of a satellite are modified strongly by the tides that operate inside the halo of the primary, it is useful to define the satellite's properties at the time of accretion, and to refer the evolution to the values measured at that time.

One example of the effect of tides is provided by the self-bound mass of the satellite, whose evolution is shown in the bottom panel of Fig. 6. The dark matter that remains bound to the satellite (relative to that measured at accretion time) is shown by open symbols; the bound mass in stars is shown by solid triangles. One of the satellites (dashed lines) sees its orbit eroded quickly by dynamical friction, and merges with the primary less than 4 Gyr after accretion, at which point the self-bound mass of the dark matter and stellar components drops to zero. The orbital period decreases rapidly as the satellite sinks in; we are able to trace almost five complete orbits before disruption although, altogether, the satellite takes only 2.5 Gyr to merge after the first pericentric passage, a time comparable to just half the orbital period at accretion time.

As the satellite is dragged inwards by dynamical friction, dark matter is lost much more readily than stars; after the first pericentric passage, only about 40 per cent of the original dark mass remains

attached to the satellite, compared with 85 per cent of the stars. This is a result of the strong spatial segregation between stars and dark matter which results from gas cooling and condensing at the centre of dark haloes before turning into stars. Stars are only lost in large numbers at the time of merger, when the satellite is fully disrupted by the tides.

The second satellite (solid lines in Fig. 6) survives as a self-bound entity until the end of the simulation. Its orbit is affected by dynamical friction, but not as drastically as the merged satellite: after completing three orbits, its apocentric distance has only dropped from ~250 kpc at turnaround ($t_{ta} \sim 3$ Gyr) to ~180 kpc at $z = 0$. The stars in the satellite survive almost unscathed; more than 85 per cent of stars remain bound to the satellite at the end of the simulation, although only ~45 per cent of the dark matter is still attached to the satellite then.

As expected from simple dynamical friction arguments, the final fate of a satellite regarding merging or survival depends mainly on its mass and on the eccentricity of its orbit. The 'merged' satellite in Fig. 6 is nearly six times more massive than the 'surviving' one and is on a much more eccentric orbit: its first pericentric radius is just ~20 kpc, compared with 45 kpc for the surviving satellite. More massive satellites on eccentric orbits spiral in faster than low-mass ones, making themselves more vulnerable to tides and full disruption.

This is confirmed in Fig. 7, where we show the orbital decay time-scale of all satellites identified in our simulations as a function of their mass. Satellite masses are shown in units of the mass of the primary galaxy at the time of accretion, and decay time-scales, τ, are normalized to the orbital period of the satellite, measured at the same time. (The time-scale τ is computed by fitting the evolution of
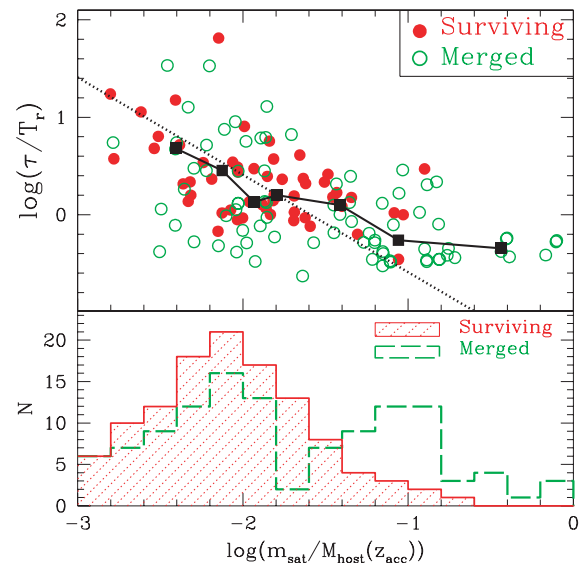

Figure 7. Top panel: orbital decay time-scale of satellites, τ, shown as a function of satellite mass. Decay time-scales are computed by fitting an exponential law to the evolution of the apocentric radius of a satellite, and is shown in units of the (radial) orbital period measured at accretion time. Satellite masses (dark+baryons) are scaled to the total mass of the host at t_{acc}. Filled and open circles correspond to satellites that have, respectively, survived or merged with the primary by $z = 0$. Filled squares show the median decay time-scale after splitting the sample into equal-number mass bins. More massive satellites spiral in faster due to the effects of dynamical friction. Bottom panel: histogram of surviving and merged satellites as a function of satellite mass. Note the strong mass bias of surviving satellites relative to merged ones.

the apocentric distance of the satellite, a good proxy for the orbital energy, to an exponential law.)

Surviving satellites are shown as filled circles in Fig. 7, whereas open circles denote merged satellites. More massive satellites clearly spiral in faster: τ is typically less than an orbital period for a satellite whose mass exceeds ~20 per cent of the primary. On the other hand, decay time-scales are often larger than ~10 orbital periods for satellites with masses below 1 per cent of the primary. The dotted line shows the $\tau \propto m^{-1}$ relation expected from simple dynamical friction arguments (Binney & Tremaine 1987). Most satellites follow this trend, except perhaps for the most massive systems, but this may just reflect difficulties estimating τ for systems on very rapidly decaying orbits, because of poor time sampling. The main result of these trends is a severe underrepresentation of surviving satellites amongst massive satellites, as shown by the distribution of satellite masses in the bottom panel of Fig. 7.

3.5.2 Orbital circularization

As they are dragged inwards by dynamical friction, the orbital energy of the satellites is affected more than its angular momentum and, as a result, the satellites' orbits become gradually more circular. This is shown in Fig. 8, where we plot the ratio between apocentric and pericentric distance, r_{per}/r_{apo}, at the time of accretion versus the same quantity, but measured after dynamical friction has eroded r_{apo} to e^{-1} of its value at accretion.

As in Fig. 7, open and filled circles indicate 'merged' and 'surviving' satellites at $z = 0$. The vast majority of the points lie above the 1:1 line, indicating that the orbits have become significantly less eccentric with time. Some points lie below the dotted line, indicat-
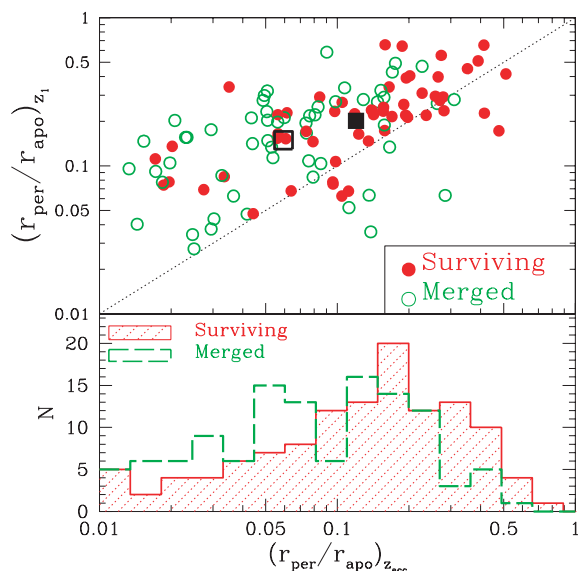

Figure 8. Top panel: orbital pericenter-to-apocenter ratio measured at two different times during the evolution of a satellite. Values on the horizontal axis correspond to the time of accretion whereas values on the vertical axis are computed once dynamical friction has eroded the apocentric distance to $\sim e^{-1}$ of its turnaround value. Most satellites lie above the 1:1 dotted line, indicating significant orbital circularization by dynamical friction. Open and filled circles correspond, respectively, to merged or surviving satellites at $z = 0$. Open and filled squares mark the median of each of those populations, respectively. Bottom panel: histogram of pericenter-to-apocenter ratio at the time of accretion for surviving and merged satellites. Note that satellites originally on more eccentric orbits tend to merge faster.

ing the opposite effect; however, most of these cases correspond to complex accretion where the satellite comes as a member of a pair of satellites and is subject to three-body interactions during accretion (see Sales et al. 2007 for further details).

The large open and filled squares indicate the median r_{per}/r_{apo} for merged and surviving satellites, respectively. Clearly, the eccentricity of the orbit is important for the chances of survival of a satellite: most satellites originally on very eccentric orbits have merged with the primary by $z = 0$, and the reverse is true for surviving satellites (see bottom panel in Fig. 8).

Satellites that merge with the primary by $z = 0$ experience on average a more substantial circularization of their orbits; the median r_{per}/r_{apo} evolves from 0.06 to roughly 0.15 in the time it takes their orbital energies to decrease by e^{-1}. Further circularization may be expected by the time that the satellite merges with the primary and, under the right circumstances, a satellite may even reach a nearly circular orbit before merging (see e.g. Abadi et al. 2003b; Meza et al. 2005).

Orbital circularization has been proposed as an important factor to consider when interpreting the effects of satellite accretion events (although see Colpi, Mayer & Governato 1999 for a different viewpoint). Abadi et al. (2003b) argue, for example, that a satellite on a circularized orbit might have contributed a significant fraction of the thick-disc stars (and perhaps even some old thin-disc stars) of the Milky Way. A further example is provided by the 'ring' of stars discovered by the SDSS in the antigalactic centre direction (Newberg et al. 2002; Helmi et al. 2003; Yanny et al. 2003), which has been successfully modelled as debris from the recent disruption of a satellite on a nearly circular orbit in the outskirts of the Galactic disc (Peñarrubia, McConnachie & Babul 2006). Since it is unlikely that the satellite formed on such orbit (otherwise it would have been disrupted much earlier), its orbit has probably evolved to become more bound and less eccentric as dynamical friction brought the satellite nearer the Galactic disc, in agreement with the trend shown in Fig. 8.

3.6 Satellites and stellar halo: similarities and differences

The main result of the trends discussed in the preceding section is the obvious mass bias present in the population of surviving satellites: massive satellites merge too quickly to be fairly represented amongst satellites present at any given time. This is shown in the bottom panel of Fig. 7; although the accretion of satellites with masses exceeding 10 per cent of the host (at the time of accretion) is not unusual, few have survived self-bound until $z = 0$.

This is also true when expressed in terms of the total stellar mass that these accretion events have contributed to the simulated galaxy. As shown in Fig. 9, merged satellites dominate the high-mass end of the distribution of accreted satellites, and make up on average ~60 per cent of all accreted stars. Half of this contribution comes in just a few massive satellites exceeding 10 per cent of the final mass in stars of the host (see upper panel in Fig. 9). On the other hand, surviving satellites contribute on average ~40 per cent of all accreted stars and have a combined stellar mass of about 12 per cent of the host at $z = 0$. Half of them are contributed by satellites less than ~3 per cent as massive as the host at $z = 0$.

Because of the strong orbital decay dependence on mass, surviving satellites are also biased relative to the overall population of accreted material in terms of accretion time. This is shown quantitatively in Fig. 10, which shows the z_{acc} distribution for all satellites accreted since $z = 4$ (top panel). The bottom and middle panels, respectively, split this sample between satellites that have either
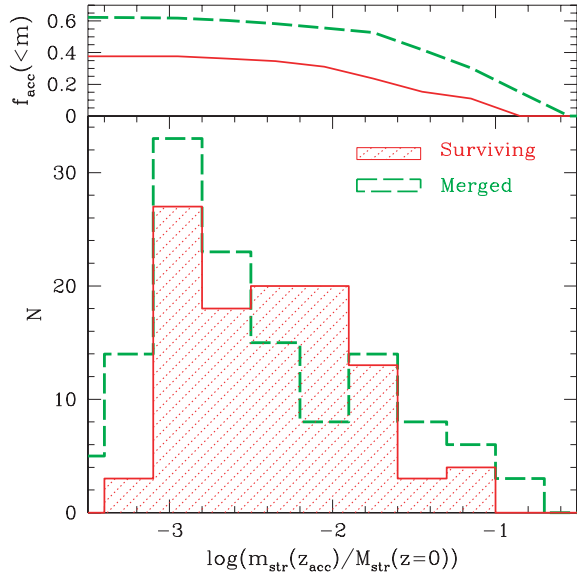
Downloaded from https://academic.oup.com/mnras/article/379/4/1464/998206 by guest on 16 August 2022

Figure 9. Distribution of satellite stellar masses measured at the time of accretion into the host halo, and normalized to the stellar mass of the primary at $z = 0$ (bottom panel). The shaded histogram corresponds to satellites that remain self-bound at $z = 0$; the other histogram corresponds to satellites that merge with the primary before $z = 0$. The curves in the top panel indicate the cumulative fraction of all *accreted stars* contributed by each of these two populations. Note that the 'building blocks' of the stellar halo are significantly more massive than the average surviving satellite. On average, accretion events bring about 25 per cent of the total number of stars into the primary, 40 per cent of which remains attached to satellites until $z = 0$. The remainder belongs to 'merged' satellites, the majority of which make up the stellar halo. The total number of stars contributed by disrupted satellites exceed those locked in surviving satellites by ~ 50 per cent.

survived or merged with the host by $z = 0$. The vertical lines in this figure illustrate the average mass accretion history of the hosts in our simulation series: from left- to right-hand side, the vertical lines indicate the average redshift when the last 25, 50 and 75 per cent of the mass were assembled into the virial radius of the host.

The accreted satellites, as a whole, trace very well this accretion history, as may be seen from the histogram in the top panel, or by the dotted line, which indicates the cumulative accretion history (scale on right). Just like the total mass, half of all satellites were accreted before $z \sim 1.8$ (see arrow labelled '50 per cent'). The results are quite different for 'merged satellites'; half of them were actually accreted before $z = 2.4$, which corresponds to a look back time of ~ 2.7 Gyr. Essentially no satellite accreted after $z = 0.5$ has merged with the primary. Surviving satellites, on the other hand, are substantially biased towards late accretion. Half of them were only accreted after $z = 1.4$, and the last 25 per cent since $z \sim 1$.

Since stars brought into the galaxy by merged satellites contribute predominantly to the stellar halo (see e.g. Abadi et al. 2006), this result shows convincingly that substantial differences must be expected between the stellar halo and surviving satellite population in a galaxy built hierarchically. *The 'building blocks' of the stellar halo were on average more massive and were accreted and disrupted much earlier than the population of satellites that survive until the present.*

Our results provide strong support for the semi-analytic modelling results of Bullock & Johnston (2005). Despite the differences in modelling techniques (these authors use theoretical merger trees to simulate Monte Carlo accretion histories and a semi-analytic ap-
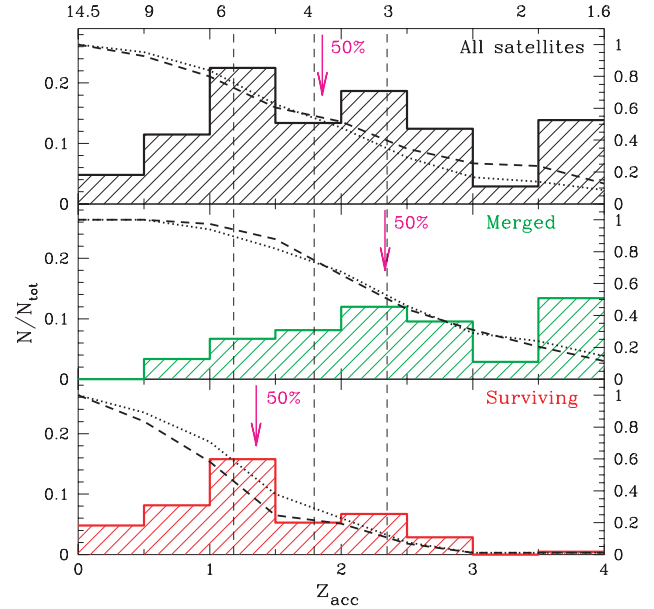

Figure 10. Accretion redshift distribution of surviving (bottom panel), merged (middle) and all (top) satellites in our simulations. All histograms are scaled to the total number of satellites for ease of comparison between panels. Dashed vertical lines indicate the (average) redshift where the primary galaxy has accreted 25, 50 and 75 per cent of its *total* mass at $z = 0$. In each panel, the arrow shows the median satellite accretion redshift. The dotted curves trace the cumulative distribution of satellites (by number) as a function of z_{acc} (scale on right-hand side). Solid lines are like dotted ones, but by mass.

proach to distinguish stars and dark matter within accreted satellites), our results agree well. For example, they find that ~ 80 per cent of the stellar halo is contributed by the ~ 15 most massive disrupted satellites; we find, on average, 70 per cent. The median accretion time for disrupted satellites is ~ 9 Gyr ago; we find ~ 10.5 Gyr. Lastly, they find that the median accretion time of surviving satellites was as recently as ~ 5 Gyr in the past; we find ~ 8.5 Gyr.

As discussed by Font et al. (2006a,b), these results may help to explain the differences between the abundance patterns of halo stars in the solar neighbourhood and in Galactic dwarfs (Fuhrmann 1998; Shetrone et al. 2001, 2003; Venn et al. 2004). Although stars in both the halo and satellites are metal-poor, the stellar halo is, at fixed [Fe/H], more enhanced in α-elements than stars in the dwarfs, suggesting that its star formation and enrichment proceeded more quickly and thoroughly than in Galactic satellites. This is qualitatively consistent with the biases in the surviving satellite population mentioned above. Because of the limited numerical resolution of our simulations and our inefficient feedback recipe, we are unable to follow accurately the metal enrichment of stars in our simulations. Although this precludes a more detailed quantitative comparison between simulations and observations, we regard the distinction between satellite and stellar halo reported here as certainly encouraging.

One final issue to consider is that, in principle, stars may also end up in the stellar halo as a result of partial stripping of surviving satellites. If substantial, this process might make stars in the stellar halo difficult to differentiate from those attached to satellites, despite the biases in mass and accretion time discussed above. As it turns out, stripping of surviving satellites adds an insignificant fraction of stars to the halo in our simulations; stars stripped from surviving satellites make up a small fraction (~ 6 per cent) of all halo stars.
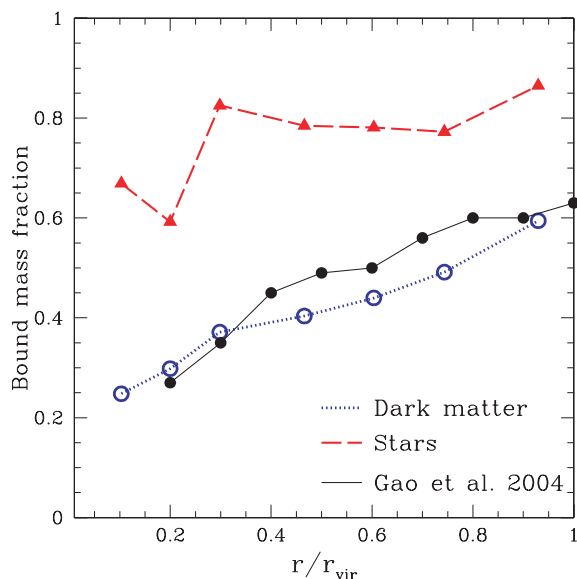
Figure 11. Mass fraction attached to surviving satellites at $z = 0$, shown as a function of radius, normalized to the virial radius of the host. The open circles are the results of the dark matter-only simulations of Gao et al. (2004), which are in very good agreement with ours. This figure shows that, although surviving satellites have lost a significant fraction of their dark mass to tides, their stellar components have survived almost unscathed. Overall, satellites inside the virial radius have conserved about 40 per cent of their original dark mass, and ∼75 per cent of their stars. This suggests that stars stripped off surviving satellites are in general an unimportant contributor to the stellar halo, and highlights the need for simulations that include gas cooling and star formation to estimate the importance of tidal stripping in the satellite population.

This is shown in Fig. 11, where we plot the fraction of stars and dark matter that remains attached to surviving satellites as a function of the distance to the centre of the galaxy. As shown by the filled triangles, more than 75 per cent of the stars brought into the system by surviving satellites remain attached to them at $z = 0$. We conclude that the bulk of the halo population is not affected by stars stripped from existing satellites, and that the substantial difference between the stellar population of Galactic dwarfs and of the stellar halo predicted above is robust.

4 SUMMARY

We have analysed the properties of satellite galaxies formed in a suite of eight *N*-body/gasdynamical simulations of galaxy formation in a ΛCDM universe. Our simulations are able to resolve, at $z = 0$, ∼10 most luminous satellites orbiting around ∼L_* galaxies. We also track satellites that have merged with, or been disrupted fully by, the primary galaxy at earlier times, giving us a full picture of the contribution of accreted stars to the various dynamical components of the galaxy.

As discussed in an earlier paper of our group (Abadi et al. 2006), the stellar halo consists of stars stripped from satellites that have been fully disrupted by the tidal field of the primary. Our analysis here focuses on the spatial distribution, kinematics and merging history of the population of surviving and merged satellites, and on their significance for the formation of the stellar halo. Our main results may be summarized as follows.

(i) The spatial distribution of satellites at $z = 0$ is consistent with that of the dark matter in the primary galaxy's halo, and is signifi-

cantly more extended than the stellar halo. On average, half of the ∼10 brightest satellites are found within $0.37 r_{\rm vir}$, comparable to the half-mass radius of the dark matter component. The half-mass radius of the stellar halo is, on the other hand, only $0.05 r_{\rm vir}$.

(ii) The kinematics of the satellite population are also similar to the dark matter's. Satellite velocities are mildly anisotropic in the radial direction, with $\beta_{\rm sat} \sim 0.3$–0.4, but not as extreme as stars in the halo, which are found to have $\beta_{\rm halo} \sim 0.6$–$0.8$ in the outskirts of the system. Satellite velocity dispersions drop from the centre outwards, and decrease by about a factor of 2 at the virial radius from their central value. Overall, the velocity dispersion of the satellite population is found to provide a reasonable estimate of the halo's virial velocity: $\sigma_{\rm sat}/V_{\rm vir} \sim 0.9 \pm 0.2$, where the uncertainty is the rms of the eight simulations.

(iii) The orbits of satellites evolve strongly after accretion as a result of dynamical friction with the host halo and of mass stripping by tides. More massive satellites spiral in faster than less massive systems and are disrupted quickly as they merge with the primary, adding their stars mainly to the stellar halo. The orbits of satellites with masses exceeding 10 per cent of the host mass decay on exponential time-scales shorter than an orbital period, and merge shortly after accretion. Merged satellites typically make up ∼63 per cent of all accreted stars in a galaxy, a substantial fraction of which (57 per cent) was contributed by these few most massive satellites.

(iv) Surviving satellites are a substantially biased tracer of the whole population of stars accreted by a galaxy. In contrast with the 'merged' satellites that build up the halo, surviving satellites are predominantly low-mass systems that have been accreted recently. Half of the stars in the stellar halo were accreted before $z \sim 2.2$, and were in satellites more massive than ∼6 per cent of the host at the time of accretion. In contrast, half of the stars in surviving satellites were brought into the system as recently as $z \sim 1.6$, and formed in systems with masses less than 3 per cent of the host.

(v) Satellite orbits are continuously circularized by dynamical friction as they orbit within the primary's halo. The pericenter-to-apocenter ratio typically doubles once the orbital binding energy of the satellite has increased by a factor of *e*.

(vi) Stars stripped from satellites that remain self-bound until the present make up an insignificant fraction of all stars accreted by a galaxy, showing that, once started, the disruption process of the stellar component of a satellite progresses on a very short time-scale. Surviving satellites conserve at $z = 0$ about 75 per cent of the stars they had at accretion time. Their surrounding dark haloes, on the other hand, have been stripped of more than ∼40 per cent of their mass.

Our results offer a framework for interpreting observations of the satellite population around luminous galaxies and for extracting information regarding their dark matter haloes. They also show that hierarchical galaxy formation models may explain naturally the differences in the properties of stars in the stellar halo and in Galactic satellites highlighted by recent observational work. Although our modelling of star formation is too simplistic (and our numerical resolution too poor) to allow for a closer, quantitative assessment of this issue, it is encouraging to see that, despite their differences, stellar haloes and satellites may actually be both the result of the many accretion events that characterize galaxy formation in a hierarchically clustering universe.

REFERENCES

Abadi M. G., Navarro J. F., Steinmetz M., Eke V. R., 2003a, ApJ, 591, 499
Abadi M. G., Navarro J. F., Steinmetz M., Eke V. R., 2003b, ApJ, 597, 21
Abadi M. G., Navarro J. F., Steinmetz M., 2006, MNRAS, 365, 747
Belokurov V., Zucker D. B., Evans N. W., Wilkinson M. I., Irwin M. J., Hodgkin S., Bramich D. M., 26 coauthors, 2006, ApJ, 647, L111
Belokurov V. et al., 2007, ApJ, 654, 897
Benson A. J., Frenk C. S., Sharples R. M., 2002a, ApJ, 574, 104
Benson A. J., Lacey C. G., Baugh C. M., Cole S., Frenk C. S., 2002b, MNRAS, 333, 156
Binney J., Tremaine S., 1987, Galactic Dynamics. Princeton Univ. Press, Princeton, NJ, p. 747
Bower R. G., Benson A. J., Malbon R., Helly J. C., Frenk C. S., Baugh C. M., Cole S., Lacey C. G., 2006, MNRAS, 370, 645
Brainerd T. G., 2004a, preprint (astro-physics e-prints)
Brainerd T. G., 2004b, in Allen R. E., Nanopoulos D. V., Pope C. N., eds, AIP Conf. Proc. 743, The New Cosmology: Conference on Strings and Cosmology. Springer Verlag, New York, p. 129
Bryan G. L., Norman M. L., 1998, ApJ, 495, 80
Bullock J. S., Johnston K. V., 2005, ApJ, 635, 931
Bullock J. S., Kravtsov A. V., Weinberg D. H., 2000, ApJ, 539, 517
Chapman S. C. et al., 2007, ApJ, 662, L79
Cole S., Aragon-Salamanca A., Frenk C. S., Navarro J. F., Zepf S. E., 1994, MNRAS, 271, 781
Cole S., Lacey C. G., Baugh C. M., Frenk C. S., 2000, MNRAS, 319, 168
Colless M. et al., 2001, MNRAS, 328, 1039
Colpi M., Mayer L., Governato F., 1999, ApJ, 525, 720
Croton D. J. et al., 2006, MNRAS, 365, 11
De Lucia G., Kauffmann G., Springel V., White S. D. M., Lanzoni B., Stoehr F., Tormen G., Yoshida N., 2004, MNRAS, 348, 333
Diemand J., Moore B., Stadel J., 2004, MNRAS, 352, 535
Font A. S., Johnston K. V., Bullock J. S., Robertson B. E., 2006a, ApJ, 638, 585
Font A. S., Johnston K. V., Bullock J. S., Robertson B. E., 2006b, ApJ, 646, 886
Fuhrmann K., 1998, A&A, 338, 161
Gao L., De Lucia G., White S. D. M., Jenkins A., 2004, MNRAS, 352, L1
Gao L., White S. D. M., Jenkins A., Stoehr F., Springel V., 2004, MNRAS, 355, 819
Ghigna S., Moore B., Governato F., Lake G., Quinn T., Stadel J., 1998, MNRAS, 300, 146
Ghigna S., Moore B., Governato F., Lake G., Quinn T., Stadel J., 2000, ApJ, 544, 616
Gilmore G., Wyse R. F. G., 1998, AJ, 116, 748
Gnedin O. Y., Weinberg D. H., Pizagno J., Prada F., Rix H.-W., 2006, preprint (astro-physics e-prints)
Hayashi E., Navarro J. F., Taylor J. E., Stadel J., Quinn T., 2003, ApJ, 584, 541
Helmi A., Navarro J. F., Meza A., Steinmetz M., Eke V. R., 2003, ApJ, 592, L25
Holmberg E., 1969, Ark. Astron., 5, 305
Ibata R., Martin N. F., Irwin M., Chapman S., Ferguson A. M. N., Lewis G. F., McConnachie A. W., 2007, ApJ, in press
Irwin M. J. et al., 2007, ApJ, 656, L13

Kauffmann G., White S. D. M., Guiderdoni B., 1993, MNRAS, 264, 201
Kazantzidis S., Mayer L., Mastropietro C., Diemand J., Stadel J., Moore B., 2004, ApJ, 608, 663
Kennicutt R. C. Jr, 1998, ApJ, 498, 541
Klypin A., Kravtsov A. V., Valenzuela O., Prada F., 1999, ApJ, 522, 82
Klypin A., Zhao H., Somerville R. S., 2002, ApJ, 573, 597
Kravtsov A. V., Gnedin O. Y., Klypin A. A., 2004, ApJ, 609, 482
Libeskind N. I., Cole S., Frenk C. S., Okamoto T., Jenkins A., 2007, MNRAS, 374, 16
Majewski S. R. et al., 2007, preprint (astro physics e-prints)
Martin N. F., Ibata R. A., Irwin M. J., Chapman S., Lewis G. F., Ferguson A. M. N., Tanvir N., McConnachie A. W., 2006, MNRAS, 371, 1983
McConnachie A. W., Irwin M. J., 2006, MNRAS, 365, 902
McKay T. A. et al., 2002, ApJ, 571, L85
Meza A., Navarro J. F., Steinmetz M., Eke V. R., 2003, ApJ, 590, 619
Meza A., Navarro J. F., Abadi M. G., Steinmetz M., 2005, MNRAS, 359, 93
Moore B., Ghigna S., Governato F., Lake G., Quinn T., Stadel J., Tozzi P., 1999, ApJ, 524, L19
Moore B., Diemand J., Madau P., Zemp M., Stadel J., 2006, MNRAS, 368, 563
Nagai D., Kravtsov A. V., 2005, ApJ, 618, 557
Navarro J. F., Abadi M. G., Steinmetz M., 2004, ApJ, 613, L41
Newberg H. J. et al., 2002, ApJ, 569, 245
Peñarrubia J., McConnachie A., Babul A., 2006, ApJ, 650, L33
Peñarrubia J., McConnachie A., Navarro J. F., 2007, preprint (astro physics e-prints)
Prada F. et al., 2003, ApJ, 598, 260
Pritzl B. J., Venn K. A., Irwin M., 2005, AJ, 130, 2140
Sales L. V., Navarro J. F., Abadi M. G., Steinmetz M., 2007, MNRAS, in press (doi:10.1111/j.1365-2966.2007.12026.x)
Searle L., Zinn R., 1978, ApJ, 225, 357
Seigar M. S., Barth A. J., Bullock J. S., 2006, preprint (astro physics e-prints)
Shetrone M. D., Côté P., Sargent W. L. W., 2001, ApJ, 548, 592
Shetrone M., Venn K. A., Tolstoy E., Primas F., Hill V., Kaufer A., 2003, AJ, 125, 684
Smith M. C. et al., 2006, preprint (astro physics e-prints)
Sofue Y., Rubin V., 2001, ARA&A, 39, 137
Somerville R. S., Primack J. R., Faber S. M., 2001, MNRAS, 320, 504
Springel V., White S. D. M., Tormen G., Kauffmann G., 2001, MNRAS, 328, 726
Steinmetz M., 1996, MNRAS, 278, 1005
Steinmetz M., Navarro J. F., 2002, New Astron., 7, 155
Stoehr F., White S. D. M., Tormen G., Springel V., 2002, MNRAS, 335, L84
Strauss M. A. et al., 2002, AJ, 124, 1810
Strigari L. E., Bullock J. S., Kaplinghat M., 2007a, ApJ, 657, L1
Strigari L. E., Kaplinghat M., Bullock J. S., 2007b, Phys. Rev. D, 75, 061303
Taylor J. E., Babul A., 2001, ApJ, 559, 716
Taylor J. E., Silk J., Babul A., 2005, in Jerjen H., Binggeli B., eds, IAU Colloq. 198: Near-fields Cosmology with Dwarf Elliptical Galaxies. Cambridge Univ. Press, Cambridge, p. 185
Unavane M., Wyse R. F. G., Gilmore G., 1996, MNRAS, 278, 727
van den Bergh S., 1999, A&AR, 9, 273
van den Bosch F. C., Weinmann S. M., Yang X., Mo H. J., Li C., Jing Y. P., 2005, MNRAS, 361, 1203
Venn K. A., Irwin M., Shetrone M. D., Tout C. A., Hill V., Tolstoy E., 2004, AJ, 128, 1177
Weinberg D. H., Colombi S., Davé R., Katz N., 2006, preprint (astro physics e-prints)
White S. D. M., Rees M. J., 1978, MNRAS, 183, 341
Willman B. et al., 2005, ApJ, 626, L85
Yanny B. et al., 2003, ApJ, 588, 824
York D. G. et al., 2000, AJ, 120, 1579
Zaritsky D., Smith R., Frenk C., White S. D. M., 1993, ApJ, 405, 464
Zaritsky D., Smith R., Frenk C., White S. D. M., 1997, ApJ, 478, 39
Zucker D. B. et al., 2004, ApJ, 612, L121
Zucker D. B. et al., 2006, ApJ, 643, L103

This paper has been typeset from a TeX/LaTeX file prepared by the author.